Published in the Proceedings of the 16th International Aluminum Alloys Conference (ICAA16) 2018
ISBN: 978-1-926872-41-4
by the Canadian Institute of Mining, Metallurgy & Petroleum

APPLICATION OF MODIFIED VOCE-KOCKS CONSTITUTIVE MATERIAL MODEL TO ELEVATED TEMPERATURE FORMING OF 7XXX SERIES ALUMINUM SHEET

Z. T. Xu[1], M. Bruhis[1], *M. K. Jain[1], and V. Hegedekatte[2]

[1]*Department of Mechanical Engineering, McMaster University*
Hamilton, Ontario, Canada
*(*Corresponding author: jainmk@mcmaster.ca)*

[2]*Novelis Global Research and Technology Center*
Kennesaw, GA, USA.

ABSTRACT

Strain rate and temperature dependent deformation conditions are present during elevated temperature forming of aluminum and other metallic materials. While many constitutive laws have been proposed to represent such deformation conditions, a closer investigation often reveals their limited applicability in terms of fit to the experimental data, and interpolation within and extrapolation outside of the range of experimental stress-strain curves. This is often because material-specific primary deformation mechanisms of temperature-dependent strain and strain rate hardening are poorly captured. In the present work, the Voce-Kocks constitutive model based on mechanics of dislocations storage and annihilation has been found to be suitable for many metallic materials. The model was modified to include the effect of temperature dependent shear modulus. The modified model is then employed to represent the experimental data obtained from uniaxial tensile tests on AA7075-O sheet at elevated temperatures and strain rates. Also, hot gas bulging tests were conducted to verify the applicability of this model. Further, finite element simulation of the hot gas bulge test was performed by incorporating the model as a user material subroutine. Good general agreement was observed between the experimental and FE model predicted results. Some sources of discrepancy in the prediction are also discussed.

KEYWORDS

7xxx aluminum sheet, Constitutive material modeling, Temperature and strain rate dependency, Hot gas bulging test

INTRODUCTION

There has been much interest in light-weighting of automobiles from automotive related industries to reduce overall carbon footprint and increase energy efficiency of the vehicles. Aluminum alloys, and especially the medium-strength 5xxx and 6xxx series alloys, have been the primary focus in the last 3 decades to reach the above environmental goals (Huo, Hou, Zhang, & Zhang, 2016) whereas aerospace industry has traditionally focused on high strength 7xxx series aluminum (Al-Zn-Mg-Cu) alloys for structural components (Deng, Yin, & Huang, 2011). Recently, there has been much interest in high strength 7xxx series aluminum as a replacement for heavier steel automotive structural parts such as A-pillar, B-pillar, side impact beams etc. (Harrison & Luckey, 2014). This is both interesting and challenging since the above aluminum structural parts will need to not only meet impact safety standards but also possess sufficient formability for manufacturing such complex parts. Since the formability of high strength 7xxx series materials is quite poor at room temperature, much interest has focused on improving both formability and final part strength via high rate hot stamping, in-die quenching, and subsequent artificial ageing process steps (Kumar & Ross, 2016).

Compared to traditional cold forming processes, sheet materials deformed under elevated temperature forming conditions are temperature and strain rate dependent (Lin & Chen, 2011). An accurate representation of large plastic deformation behavior of 7xxx series aluminum alloys under different temperatures and strain rate conditions is thus one of the fundamental issues to be addressed for the successful application of the elevated temperature forming processes. From a practical and phenomenological standpoint, a balanced approach that incorporates the essence of most relevant or significant mechanism(s) for capturing the constitutive behavior of 7xxx aluminum alloys in the range of temperatures and strain rates of interest in sheet stamping is needed.

Regarding the rate and temperature dependent constitutive hardening behavior of metals and alloys in general, a number of well accepted models exist in the literatures as reviewed by Lin and Chen (2011). Among these models, the Voce-Kocks (V-K) model (Kocks, 1976; Voce, 1948) is considered a promising model for its clear physical background, reasonable fit to data, extrapolation to larger strains, and simpler formulation. Voce (1948) found that the stress-strain curves of many metals can be represented by an exponential approach to a saturation stress over a large range of strains. The Voce model was further extended by Kocks to describe the temperature and strain-rate dependence. In addition to that, Kocks was able to establish the physical mechanism of dislocation storage and dynamic recovery behind the Voce formulation. The model was then widely employed in further investigations on the temperature dependent hardening behavior of metals and alloys. In the analytical modeling scenario, more detailed descriptions were then performed in the works of Mecking and Kocks (1981) and Estrin and Mecking (1984) by relating the strain rate and stress with the description of a unique structural parameter that determines the mechanical state of material. Based on their studies, the V-K model was further assessed for its applicability to various aluminum alloys such as 3003-O, 2008-O, 5032-T4, 7449-T7651, Al-Si alloys (Barlat, Glazov, Brem, & Lege, 2002; Fribourg, Bréchet, Deschamps, & Simar, 2011; Sjölander & Seifeddine, 2013), and boron steel at high temperatures (Naderi, Durrenberger, Molinari, & Bleck, 2008).

In the derivation of the V-K model, the activation energy of dislocation motion is considered to be proportional to the shear modulus of the material (Kocks, 2001), which is in accordance with the dislocation theory (François, Pineau, & Zaoui, 1998). In many previous studies on the V-K model, the shear modulus is treated as a temperature-independent factor. However, according to Ashby (1972) the shear modulus is actually sensitive to the variation in temperature. Hence, the present work attempts to explore a modification of the V-K model with a consideration of the effect of temperature dependent shear modulus.

DISCUSSION ON THE CONSTITUTIVE HARDENING BEHAVIORS OFAA7075-O

Experiments and Analysis

To investigate the elevated forming behavior of AA7075-O sheet, uniaxial tensile tests were first conducted at different temperatures and loading speeds. As-fabricated AA7075 sheet of 2 mm thickness was received from Novelis. Uniaxial tensile samples were fabricated as per ASTM E2448-11 standard by water jet cutting, deburring, and then annealing to O-temper state by heating the samples to 428 $^{\circ}C$ at a rate of 10 $^{\circ}C/s$ in an environmental chamber, holding the samples for three hours, and finally furnace cooling to room temperature over 24 hours. The specimen geometry and uniaxial test fixture are shown in Figure 1.

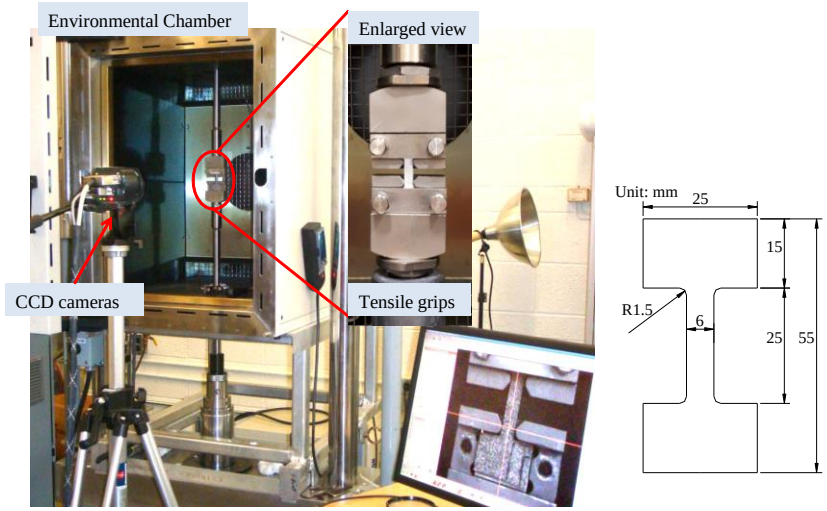

Figure 1. Uniaxial tensile test apparatus.

The specimens were tested with a computer-controlled uniaxial servo-hydraulic mechanical test system from MTS that was fitted with an environmental chamber from Instron. During the test, a digital image correlation (DIC) system, ARAMIS from GoM (Techniques GoM, 2005), was employed to continuously measure full-field strain from the gauge region of the deforming sample.

Application of V-K Model to AA7075-O Experimental Data

The V-K model is applied to elevated temperature AA7075-O uniaxial tensile test data to explore its applicability to this alloy system. The V-K model (Estrin & Mecking, 1984; Kocks, 1976; Voce, 1948) was derived based on the concept of dislocation behavior during the plastic deformation in hot working. As the deformation increases, the plastic flow leads to a rise in the dislocation density and thus an increased resistance to the motion of dislocations. Hence, an increase in flow stress with applied strain, also referred as plastic work or strain hardening, occurs. Also, under elevated temperature conditions, some annihilation and rearrangement of dislocations, referred as the dislocation recovery or flow softening, also occurs. This latter mechanism contributes to a reduction in flow stress. The shape of the flow stress-strain curve thus depends upon the parameters that govern the kinetics of the strain hardening and flow softening processes. In the following only the final formulation of V-K model is presented. The details of derivation can be found in the previously mentioned literatures. The Voce model can be written as follows:

$$\sigma = \sigma_s + \left(\sigma_0 - \sigma_s\right)\exp\left(-\frac{\varepsilon}{\varepsilon_r}\right) \tag{1}$$

Kocks (1976) further proposed a description for the saturation stress σ_s as a function of temperature and strain rate as follows:

$$\sigma_s = \sigma_{s0}\left(\frac{\dot{\varepsilon}}{\dot{\varepsilon}_{s0}}\right)^{kT/A_s} \tag{2}$$

where k, $\dot{\varepsilon}_{s0}$ and σ_{s0} are Boltzmann constant, reference saturation strain rate (a material constant) and reference saturation stress at zero $^{\circ}K$, respectively. Furthermore, similar to the saturation stress, σ_s, the initial yield stress σ_0 can be written as:

$$\sigma_0 = \sigma_{k0}\left(\frac{\dot{\varepsilon}}{\dot{\varepsilon}_{k0}}\right)^{kT/A_k} \tag{3}$$

In addition, the characteristic strain ε_r can be expressed as (Lin & Chen, 2011; Naderi et al., 2008):

$$\varepsilon_r = \frac{\sigma_s - \sigma_0}{\theta_0} \tag{4}$$

where θ_0 is a material constant. The set of eqns. (1-4) represents the temperature and strain rate dependent constitutive relationship of V-K model. The parameter values of V-K model were obtained by a two-step process, where step 1 involved least square fitting of eqn. (1) to all experimental true stress-strain data to obtain discrete values of σ_0, σ_s and ε_r at different temperatures and strain rates, and step 2 involved determining the fitting parameters in Eqns. (2-4) that relate σ_0, σ_s and ε_r to the various temperatures and strain rates. It should be noted that the room temperature ($293\ ^{\circ}K$) stress-strain data were not included in the first trial calculation of σ_s, σ_0 and ε_r. The reasons are explored and addressed in a later discussion. The experimental and predicted true stress-true strain curves are summarized in Figure 2. The calculated parameters are listed in Table 1. A comparison of σ_s and σ_0 from steps 1 and 2 are shown in Figure 3 (a,b), respectively.

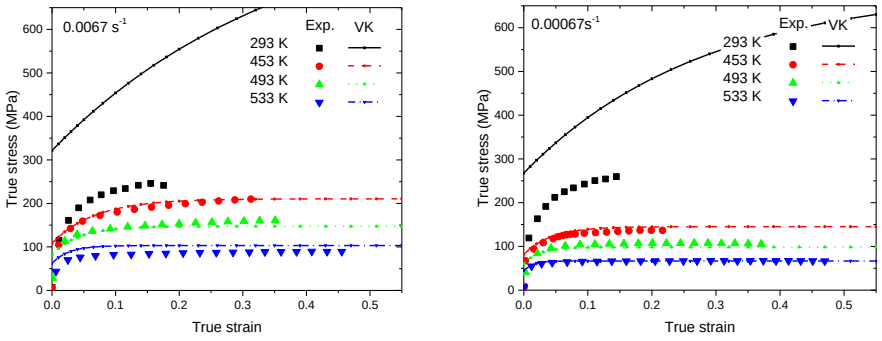

(a) (b)

Figure 2. Comparison of fitted and experimental stress-strain curves by using V-K model, (a) 0.0067 s^{-1}; (b) 0.00067 s^{-1}.

Table 1. Fitted parameters of V-K model.

σ_{s0}	y_s	A_s	σ_{k0}	y_k	A_k	θ
1.193E4	4.740E+08	3.868E-20	2.352E3	4.610E+08	5.072E-20	1.510E3

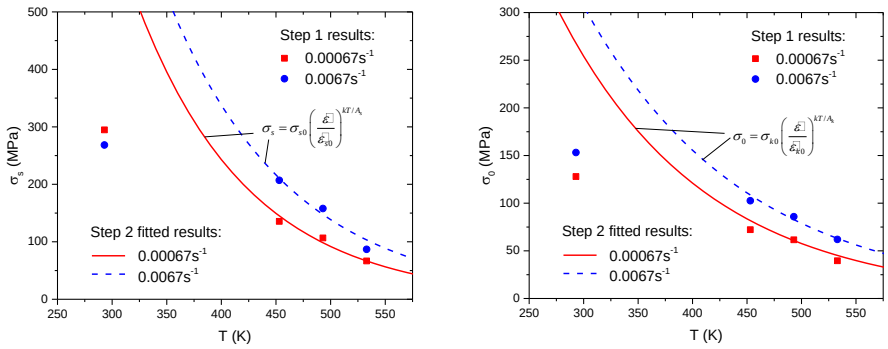

Figure 3. Results from steps 1 and 2 for, (a) σ_s, and (b) σ_0.

It can be observed that the V-K model is able to reasonably characterize the flow stress of AA7075-O sheet at elevated temperatures. However, significant overestimation of saturation and initial yield stresses (σ_s and σ_0) can be observed for the room temperature ($293\,°K$) condition. One of the possible reasons is that A_s and A_k are taken as constants in the calculation. However, they are temperature dependent factors. According to Kocks (1976), A_s and A_k are in proportion to μb^3 where μ is the shear modulus and b is the Burger's vector. In fact, μ decreases with the increase in temperature (Ashby, 1972). As a result, the calculation method above can work well for a certain temperature range, i.e., for the higher temperatures in the present experiments. However, the calculated parameters may lose accuracy if the temperature is well out of the range such as for the $293\,°K$ case due to the variation of A_s and A_k with temperature.

Modified V-K Model with Consideration of Temperature-dependent Shear Modulus

To address the problem discussed above, the expressions for σ_s and σ_0 were modified by defining a new temperature-dependent shear modulus. According to Ashby, the temperature dependent shear modulus μ can be described by the following equation:

$$m = -\frac{1}{\mu}\frac{d\mu}{dT} \tag{5}$$

where m is a material constant with a value of 5.4×10^{-4} s^{-1} for pure aluminum (Ashby, 1972). However, the m value for AA7075-O could be different. Hence m is taken as a parameter whose value is yet to be determined. From the integration of Eqn. (5), one obtains:

$$\mu = \mu_0 \exp(-mT) \tag{6}$$

where μ_0 is the shear modulus at $0\,°K$. Therefore the saturation stress σ_s can be formulated as follows:

$$\sigma_s = \sigma_{s0}\left(\frac{\dot{\varepsilon}}{\dot{\varepsilon}_{s0}}\right)^{\frac{kT}{A_s}} = \sigma_{s0}\left(\frac{\dot{\varepsilon}}{\dot{\varepsilon}_{s0}}\right)^{\frac{kT}{a_s\mu_0 b^3\exp(-mT)}} = \sigma_{s0}\left(\frac{\dot{\varepsilon}}{\dot{\varepsilon}_{s0}}\right)^{\frac{kT}{A'_s\exp(-mT)}} \tag{7}$$

Similarly, the initial yield stress σ_0 can be written as:

$$\sigma_0 = \sigma_{k0}\left(\frac{\dot{\varepsilon}}{\dot{\varepsilon}_{k0}}\right)^{\frac{kT}{A'_k\exp(-mT)}} \tag{8}$$

Eqns. (7) and (8) were then utilized to describe the effects of temperature and strain rate on σ_s and σ_0. The least square method was once again used to obtain the optimized parameter values, which are summarized in Table 2. The temperature dependency of σ_s and σ_0 from modified V-K model based on Eqns. (7) and (8) is compared with that calculated from the original V-K model in Figure 4.

Table 2. The fitted parameters of the modified V-K model.

σ_{s0}	y_s	A'_s	m	σ_{k0}	y_k	A'_k	θ
6.821E3	9.867E+02	1.020E-19	1.752E-03	2.463E03	9.950	1.018E-19	1.510E3

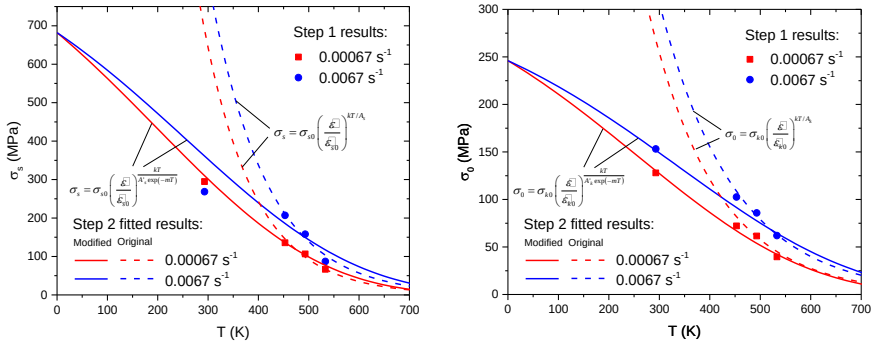

Figure 4. Comparison of σ_s and σ_0 versus temperature curves based on original and modified V-K models, (a) σ_s and (b) σ_0.

It can be observed that the modified version is able to give closer estimation of σ_s and σ_0, especially at room temperature. Nevertheless, the accuracy of σ_s for the case with the temperature of $293\,°K$ and the strain rate of 0.0067 s^{-1} is still not satisfactory. This could be attributed to early failure of tensile samples at room temperature. As a result, the uniaxial tensile results only reflect a limited portion of the hardening curve (typically less than a true strain of 0.2, as observed in Figure 5). The estimated σ_s after step 1 based on the Voce equation thus might not be quite accurate. In addition, the fitted σ_s at the temperature and strain rate of $533\,°K$ and 0.0067 s^{-1}, respectively after step 2 also deviates from that calculated from step 1, which implies that the model parameters tend to overestimate the saturation stress for this condition. On the one hand, the less accurate room temperature results of σ_s might affect the shape of fitted curves, which leads to some deterioration in the predicted stress-strain curves for the other conditions. It is also possible that AA7075-O sheet is extremely sensitive to the temperature-related experimental factors such as the heating rate, sample mounting time in the grips with the furnace open, and furnace reheating time, etc. The slight differences in these factors could easily lead to experimental error. Although the same procedure has been followed in the experiments, the error could still be induced especially for the higher temperature conditions since the loss of temperature when mounting uniaxial samples becomes more evident. Therefore, the experimental error could also account for the less accurate prediction results. A comparison of experimental results and the analytical curves based on the modified V-K model is shown in Figure 5.

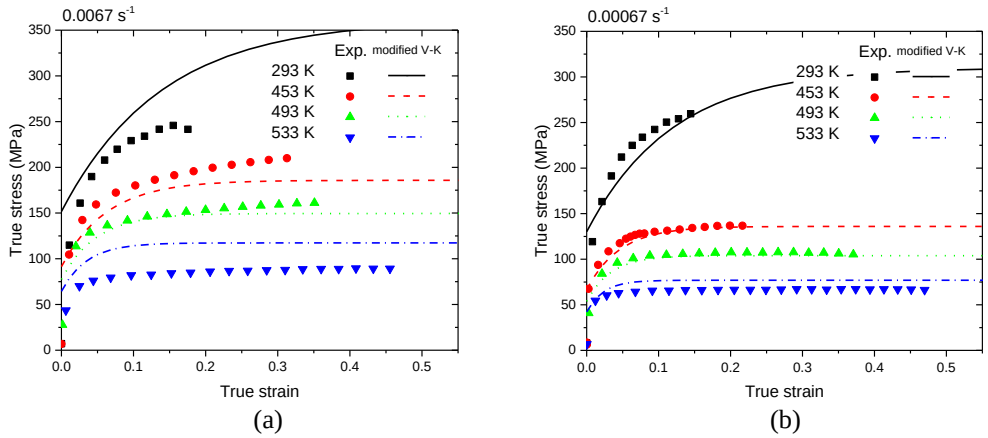

Figure 5. Comparison of fitted and experimental stress-strain curves by using the modified V-K model, (a) 0.0067 s^{-1}, and (b) 0.00067 s^{-1}.

It can be observed that the modified V-K model is able to describe the material behavior at the lower temperature of 293 $°K$. However, the accuracy for the results with the strain rate of 0.0067 s^{-1} and temperatures of 293 $°K$ and 533 $°K$ were not satisfactory compared to the other test conditions. The errors in describing the temperature and strain rate dependency of σ_s at the above two temperatures is likely the major reason. Therefore, it is important to obtain the accurate σ_s results from experiments in the first place and to describe its variation with temperature and strain rates in the future. In addition, the modified V-K model is derived based on the consideration of temperature-dependent shear modulus. Hence, experimental characterization of Young's modulus and shear modulus of AA7075-O sheet at different temperatures should be also considered in the future.

HOT GAS BULGING SIMULATION AND VERIFICATION

Modified V-K model was applied towards an analysis of the hot gas bulge tests on AA7075-O sheet. For this purpose, hot gas bulging test was conducted at 743 $°K$ and the modified V-K model was implemented as a user material subroutine (UMAT) in ABAQUS/Standard FE code. The experimental results and FE analysis of hot bulge tests are presented below.

Experimental Details of Hot Gas Bulging Tests

The hot gas bulging experimental set-up consisted of a large servo-hydraulic press of 150 Ton capacity from Macrodyne, a dedicated environmental chamber around the test bed of the press, and a gas bulging die set that was installed on the press bed and within the environmental chamber (see Figure 6). The die set consisted of a circular upper die with an open cavity at its center and a circular lock bead, and a matching circular lower die. The blank was clamped between the two dies with the lock beads by applying a suitable clamping pressure. Pressurized gas was passed through a copper tubing in to the lower die cavity to bulge the test specimen. A commercially available two-camera full-field optical strain measurement system, ARAMIS from GoM, was mounted outside of the environmental chamber, but directly above it, in the central column region of the press. The cameras were able to record the images of the deforming bulge specimen up to the onset of fracture from an opening at the top of the environmental chamber. These images were later analyzed using an integrated DIC software with the ARAMIS system to obtain curvature of the bulge in the vicinity of the pole as well as equi-biaxial strains in the pole region. Prior to the test, the environmental chamber was heated to the desired test temperature using the temperature control system of the press. A rectangular shaped AA7075-O sheet sample, with a fine speckle pattern applied to its top viewing surface, was then placed between the upper and lower dies. A thermocouple was attached to the sample to monitor its temperature. As soon as the desired temperature in sheet sample was reached, a

clamping force was applied to clamp the blank, and subsequently, the air pressure was applied at a constant pressure rate to bulge the specimen up to the onset of fracture using the control and data acquisition system of the press. The bulging test was conducted at 743 $°K$ with a pressure rate of 1 psi/s. The 3D shape of sample before and after deformation are also shown in Figure 6. The dome height versus pressure curve is presented in Figure 7 (a).

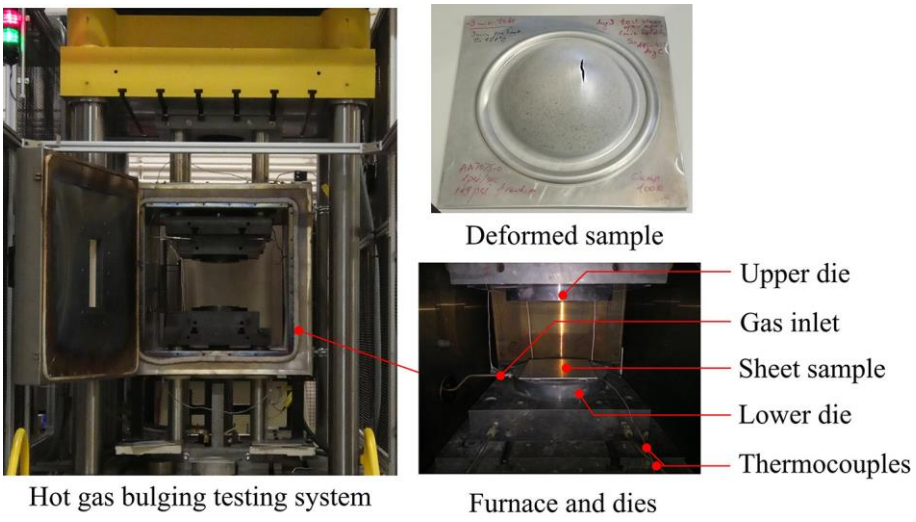

Figure 6. The hot gas bulge testing system.

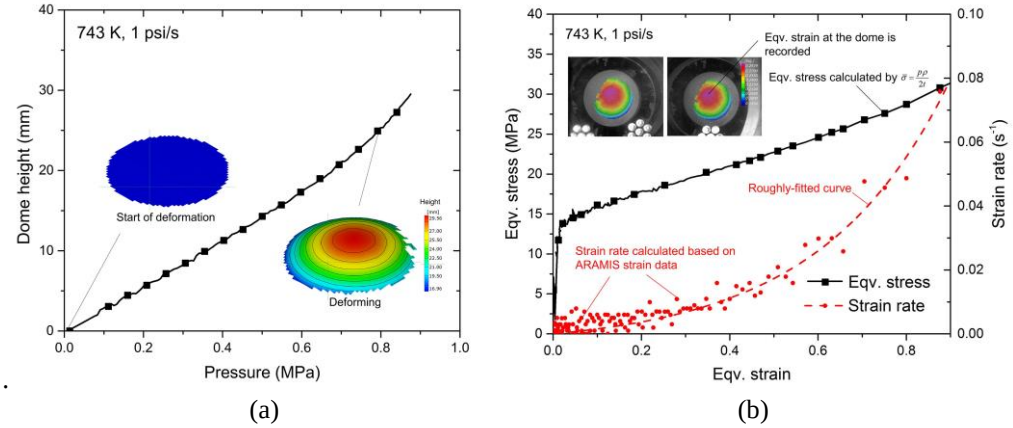

(a) (b)

Figure 7. The experimental results of gas bulge test: (a) dome height versus pressure and (b) equivalent stress and strain rate versus equivalent strain curves.

The procedure for obtaining biaxial true stress-true strain curves from bulge tests is well established, see (Gutscher, Wu, Ngaile, & Altan, 2004). It requires continuous measurements of applied pressure, bulge curvature, and principal strains in the pole region, all of the quantities as a function of time up to the onset of fracture. The equivalent stress in the pole region can be estimated by the following equation:

$$\bar{\sigma} = \frac{p\rho}{2t} \tag{9}$$

where p, ρ and t are the applied pressure, radius of curvature and current thickness at the pole of the bulge. Based on the 3D topography recorded by the ARAMIS system, the radius ρ can be obtained from 3D images of the evolving bulge surface by the ARAMIS system. The acquired camera images of the bulge surface from the ARAMIS system can also be analyzed to obtain major and minor strains in the pole region of the bulge, and consequently, the through-thickness strain based on the assumption of conservation of volume. The current thickness t can then be determined based on the through-thickness strain. Therefore, the equivalent stress and equivalent strain at the pole of the bulge can be calculated at any stage of the bulging process. Also, an approximate strain rate can be calculated from a series of recorded images of the bulging specimens at different times (i.e., from continuous strain versus time test data). The equivalent biaxial true stress versus strain and strain rate versus equivalent strain data points for AA7075-O sheet tested at 743 $^{\circ}K$ are shown in Figure 7 (b). It can be observed that the stresses increase steadily with strain during the bulging process. This is different from the uniaxial tension results which usually feature saturation in stress and even a reduction in flow stress with increase in strain at later stages, especially at high temperatures. One of the possible reasons might be the different strain rates during the uniaxial and biaxial (bulge) testing conditions. According to Dieter and Bacon (1986), the strain rate during the uniaxial tensile test can be estimated by $\dot{\varepsilon} = v/L$ where v is the test speed and L is the current gauge length of the test specimen. Since the length of sample gradually increases, the strain rate in uniaxial tensile test decreases as the specimen deforms in uniaxial tension. However, the strain rate in the present bulging test which is deformed at a constant pressure rate increases gradually as revealed in Figure 7 (b). Also, at elevated temperatures, the AA7075 sheet exhibits significant strain rate sensitivity (Jenab & Karimi Taheri, 2014). The continuously increasing strain rate thus could lead to a continuous increase in the flow stress all the way up to fracture of the bulge specimen.

Bulge Simulation Results and Discussion

As mentioned previously, the modified V-K hardening model presented previously was coded as a UMAT subroutine and incorporated into FE code ABAQUS to simulate the experimental hot gas bulging test. The FE model was set-up as a 2D-axisymmetric model for computational efficiency with the geometrical and process parameters from the bulging experiments. The AA7075-O sheet was placed between the upper and lower dies and meshed with CAX4 elements in ABAQUS/Standard. The dies were treated as discrete rigid parts. By fixing the lower die and moving the upper die downward, the AA7075-O sheet sample was first clamped prior to bulging, as in the experiments. The pressure was applied at a constant rate of 1 psi/s, same as in the experiments. The FE simulation employed the modified V-K model parameters values presented earlier in Table 2 based on uniaxial tensile tests data. The simulation and experimental results are compared in Figure 8.

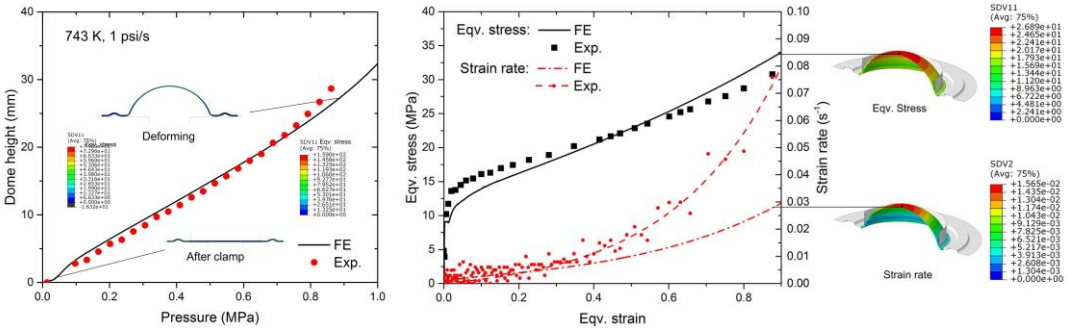

Figure 8. Compare of FE simulation and experiment results: (a) dome height versus pressure and (b) equivalent stress and strain rate versus equivalent strain curves.

The dome height versus pressure curves from FE simulation and experiment are in good general agreement, although the model curve does rise more slowly compared to the experimental curve at large

pressures closer to fracture. This underestimate of model dome height could be partially attributed to local necking and ductile damage processes that might have started in the experiments as the pressure increased to about 0.8 MPa. Since the necking and ductile damage induced failure were not included in the FE simulation, the simulation failed to estimate the deformation behavior all the way up to fracture of the specimen with accuracy. In addition, the equivalent stress versus strain and strain rate versus strain data at the pole of the bulge in the FE simulation were also recorded and compared with the experiments (see Figure 8 (b)). It can be observed that the FE simulation based on the modified V-K model yields a continuously rising stress-strain curve during the bulge test. The predicted stress and strain rate are also within acceptable range up to a strain of 0.6.

The modified V-K model is thus verified to be a suitable solution for describing the temperature and strain rate dependent constitutive behavior of AA7075-O sheet metals under various loading conditions. However, it can also be seen that the simulation underestimates the strain rate evidently as the equivalent strain increases to over 0.6. Additionally, the FE flow stress is higher than the experimental one even though the strain rate is underestimated. Hence, it is found that the fitted parameters tend to overestimate the strain rate sensitivity of AA7075-O sheet samples. This could be because the parameters of the V-K model were calculated based on the uniaxial tensile results of limited temperature and strain rate ranges. The extrapolation of both temperature and strain rate conditions to the hot bulging test at 743 $^{\circ}K$ and elevated strain rates could amplify the prediction error. Therefore, more experimental investigations regarding extended conditions of temperature and strain rate of both uniaxial tensile and biaxial bulging tests are required to further explore the constitutive behavior of AA7075-O sheet metals as well as the applicability of the presented model in this work. In addition, the variation of strain rate could lead to the uneven heat generation of plastic deformation, which could influence the flow stress during deformation. However, this effect was not included in the modeling. Hence further improvement of this model is still required to address these issues.

CONCLUSIONS

To characterize the temperature and strain rate dependent deformation behavior of AA7075-O sheet at elevated temperatures, the V-K model was modified by considering the temperature-dependent shear modulus. Both elevated temperature uniaxial tensile and gas bulging tests were employed to explore the applicability of this model. The following conclusions can be made from the present work:

1) The original and modified V-K models were employed to represent the uniaxial tensile flow behaviors of AA7075-O sheet metals at different temperatures and strain rates. The modified V-K model was found to be able to describe the plastic behaviors over a wider range of temperatures.
2) Equivalent stress-strain curve from hot gas bulging tests show a steady increase in the flow stress up to large strains without saturation at elevated temperatures. This trend is different from the uniaxial test observations which exhibit stress saturation at large strains. This difference is attributed to continuously increasing strain rate during the bulging test in a constant pressure rate test, and associated change in the strain rate sensitivity of the material during the test.
3) The modified V-K model was incorporated into a FE code to simulate the hot bulging test. By using the model parameters determined from the uniaxial tensile test data, and the FE simulations, the resulting model dome height-pressure and equivalent stress-strain curves were shown to predict the experimental trends. A number of additional factors have been identified to further assess the usefulness of the modified V-K model for accurately characterizing the hardening behavior of AA7075-O sheet metals at a wider range of temperatures and strain rates.

REFERENCES

Ashby, M. F. (1972). A first report on deformation-mechanism maps. *Acta Metallurgica, 20*(7), 887-897.

Barlat, F., Glazov, M. V., Brem, J. C., & Lege, D. J. (2002). A simple model for dislocation behavior, strain and strain rate hardening evolution in deforming aluminum alloys. *International Journal of Plasticity, 18*(7), 919-939.

Deng, Y., Yin, Z., & Huang, J. (2011). Hot deformation behavior and microstructural evolution of homogenized 7050 aluminum alloy during compression at elevated temperature. *Materials Science and Engineering: A, 528*(3), 1780-1786.

Dieter, G. E., & Bacon, D. J. (1986). *Mechanical metallurgy* (Vol. 3): McGraw-hill New York.

Estrin, Y., & Mecking, H. (1984). A unified phenomenological description of work hardening and creep based on one-parameter models. *Acta Metallurgica, 32*(1), 57-70.

François, D., Pineau, A., & Zaoui, A. (1998). *Mechanical behaviour of materials*: Springer.

Fribourg, G., Bréchet, Y., Deschamps, A., & Simar, A. (2011). Microstructure-based modelling of isotropic and kinematic strain hardening in a precipitation-hardened aluminium alloy. *Acta Materialia, 59*(9), 3621-3635.

Gutscher, G., Wu, H.-C., Ngaile, G., & Altan, T. (2004). Determination of flow stress for sheet metal forming using the viscous pressure bulge (VPB) test. *Journal of Materials Processing Technology, 146*(1), 1-7.

Harrison, N. R., & Luckey, S. G. (2014). Hot Stamping of a B-Pillar Outer from High Strength Aluminum Sheet AA7075. *SAE Int. J. Mater. Manf., 7*(3), 567-573.

Huo, W., Hou, L., Zhang, Y., & Zhang, J. (2016). Warm formability and post-forming microstructure/property of high-strength AA 7075-T6 Al alloy. *Materials Science and Engineering: A, 675*(Supplement C), 44-54.

Jenab, A., & Karimi Taheri, A. (2014). Experimental investigation of the hot deformation behavior of AA7075: Development and comparison of flow localization parameter and dynamic material model processing maps. *International Journal of Mechanical Sciences, 78*(Supplement C), 97-105.

Kocks, U. F. (1976). Laws for Work-Hardening and Low-Temperature Creep. *Journal of Engineering Materials and Technology, 98*(1), 76-85.

Kocks, U. F. (2001). Realistic constitutive relations for metal plasticity. *Materials Science and Engineering: A, 317*(1–2), 181-187.

Kumar, M., & Ross, N. G. (2016). Influence of temper on the performance of a high-strength Al–Zn–Mg alloy sheet in the warm forming processing chain. *Journal of Materials Processing Technology, 231*(Supplement C), 189-198.

Lin, Y. C., & Chen, X.-M. (2011). A critical review of experimental results and constitutive descriptions for metals and alloys in hot working. *Materials & Design, 32*(4), 1733-1759.

Mecking, H., & Kocks, U. F. (1981). Kinetics of flow and strain-hardening. *Acta Metallurgica, 29*(11), 1865-1875.

Naderi, M., Durrenberger, L., Molinari, A., & Bleck, W. (2008). Constitutive relationships for 22MnB5 boron steel deformed isothermally at high temperatures. *Materials Science and Engineering: A, 478*(1–2), 130-139.

Sjölander, E., & Seifeddine, S. (2013). Influence of alloy composition, solidification rate and artificial aging on plastic deformation behaviour of Al–Si–Cu–Mg casting alloys. *International Journal of Cast Metals Research, 26*(1), 28-36.

Techniques GoM (2005). ARAMIS v5.4 user manual. *GoM mbH*.

Voce, E. (1948). The relationship between stress and strain for homogeneous deformation. *J Inst Met, 74*, 537-562.